Inversion doublets of $3N + N$ cluster structure in excited states of ^{4}He

W. Horiuchi[1] and Y. Suzuki[2]

[1]*Graduate School of Science and Technology, Niigata University, Niigata 950-2181, Japan*

[2]*Department of Physics, and Graduate School of Science and Technology, Niigata University, Niigata 950-2181, Japan*

(Received 7 April 2008; revised manuscript received 9 July 2008; published 4 September 2008)

Excited states of ^{4}He are studied in four-body calculations with explicitly correlated Gaussian bases. All the levels below $E_x = 26$ MeV are reproduced reasonably well using realistic potentials. An analysis is made to show how the 0_2^+ state becomes a resonance but those having almost the same structure as this state in different spin-isospin channels are not observed as resonances. The role of tensor force is stressed with a particular attention to the level spacing between the two 0^- states. The calculation of spectroscopic amplitudes, nucleon decay widths, and spin-dipole transition strengths demonstrates that the 0_2^+ state and the three lowest-lying negative-parity states with 0^- and 2^- have $^3\mathrm{H} + p$ and $^3\mathrm{He} + n$ cluster configurations, leading to the interpretation that these negative-parity states are the inversion-doublet partners of the 0_2^+ state.

DOI: 10.1103/PhysRevC.78.034305 PACS number(s): 27.10.+h, 21.10.Jx, 21.45.−v, 21.60.De

I. INTRODUCTION

The competition of particle-hole and cluster excitations is one of the most interesting issues in the structure of light nuclei. They emphasize different aspects of nuclear excitation modes and often coexist in the low-lying spectrum. These excitations are usually described in quite different languages, thus defying the reproduction of such a coexistence in a single scheme. In fact, some intruder states have still not been reproduced even in large-space calculations based on realistic interactions. For example, the excitation energy of the so-called Hoyle state, which is recognized to have large overlap with 3α configuration [1], is predicted too high in the no-core shell model [2]. According to the shell model, negative-parity states should appear first in the excited spectrum of ^{16}O, but they show up just above the first excited 0^+ state, which is also understandable from $^{12}\mathrm{C} + \alpha$ structure [3].

The ^{4}He nucleus is the lightest system offering the coexistence of both particle-hole and cluster excitations in its spectrum. Its ground state is doubly magic and tightly bound, but its first excited state is not a negative parity but 0^+, as in the case of ^{16}O. This state was first conjectured as a breathing mode, but an extensive study has confirmed it as a cluster state of $3N + N$ ($^3\mathrm{H} + p$ and $^3\mathrm{He} + n$) configuration [4]. Accepting this interpretation for this state, we are led to the following questions. Because the $3N$ and N clusters having spin 1/2 and isospin 1/2 move in a relative S wave, four states may appear that all have basically the same $3N + N$ configuration but different $J^\pi T$ with $0^+0, 1^+0, 0^+1, 1^+1$. These states may be called quartet states. The first question we set here is "Why do we actually observe only one of them, 0^+0?"

The second question is concerned with the concept of an inversion doublet that is known in molecular spectroscopy. For a system consisting of asymmetric molecules (clusters), one may expect a partner state of negative parity as in the ammonia molecule. These positive- and negative-parity pairs are called inversion doublets. In analogy to the molecular case, we may ask the question "What about the possibility of observing negative-parity partners in which the $3N$ and N clusters move in a relative P wave?" The negative-parity partners would have $J^\pi = 0^-, 1^-$, and/or 2^-, which result from the coupling of the spins of the two clusters and the relative orbital angular momentum between them. The centrifugal barrier for the P wave is more than 3 MeV at the $3N$-N relative distance of 4 fm, so that the expected partner states may appear in the region of the excitation energy $E_x = 21$–23 MeV. In fact, the 0^- and 2^- states are observed in this region. Traditionally, these states are considered s^3p shell-model states, but could be better understood from the $3N + N$ configuration. A variational calculation incorporating two-body correlations explicitly seems to suggest this picture for the negative-parity states [5] but no discussion was given on the relationship between them and the 0_2^+0 state. According to recent large-space shell-model calculations, these $0^\pm0$ states show quite different convergence [6] and, because of its slow convergence, the 0_2^+0 state is attributed to a radial excitation.

The purpose of this study is to answer the two questions by performing four-body calculations with realistic potentials. Thus we are mainly interested in the three excited states 0^+0 ($E_x = 20.21$ MeV), 0^-0 (21.01 MeV), and 2^-0 (21.84 MeV), but also consider other excited states that all have widths larger than 5 MeV. We do not invoke any model ansatz; that is, our calculation is based on neither the shell model nor a resonating-group-method (RGM) calculation [7,8] that couples $^3\mathrm{H} + p$, $^3\mathrm{He} + n$, and $d + d$ two-cluster channels, but treats the four nucleons equally in a sufficiently large configuration space. We obtain the energies and wave functions of the excited states of ^{4}He using a basis expansion method. The basis used here is square integrable, so that the excited states are obtained in a bound-state approximation. As we show later, this approximation works fairly well for predicting the three lowest-lying excited states, but it gives only a qualitative prediction for the other broad levels.

Section II gives a brief description of the basis functions used to solve the four-body problem. Section III presents the results of calculation together with some discussion. We show the energy spectrum of ^{4}He in Sec. III A, discuss the problem relating to the quartet in Sec. III B, and answer the question

concerning the inversion doublets in Sec. III C. Section IV summarizes the results of the present work.

II. FORMULATION

The Hamiltonian H for a system of two protons and two neutrons consists of the kinetic energy (T) and a nucleon-nucleon potential including the Coulomb potential ($V_{\rm Coul}$). The center of mass kinetic energy is properly subtracted. A three-body force is ignored as it has a small effect on the spectrum above the $3N + N$ threshold [9]. We thus believe that its inclusion would not change the basic features concerning the structure of the ^{4}He excited states studied here. For the two-nucleon interaction we use the G3RS [10] and AV8′ [11] potential models. Both of them contain central (V_c), tensor (V_t) and spin-orbit (V_b) terms. The $\boldsymbol{L}^2$ and $(\boldsymbol{L}\cdot\boldsymbol{S})^2$ terms of the G3RS potential are ignored. The ground-state properties of d, ^{3}H, ^{3}He, and ^{4}He given by these potentials are similar to each other [12]. The tensor and spin-orbit forces of the AV8′ potential are, however, stronger than those of the G3RS potential, while the central force of the AV8′ potential is weaker than that of the G3RS potential.

A variational solution $\Psi_{JM_JTM_T}$ for the Schrödinger equation is obtained by taking a linear combination of many basis states, each of which has the form

$$\Phi_{(LS)JM_JTM_T} = \mathcal{A}\left\{e^{-\frac{1}{2}\tilde{\boldsymbol{x}}A\boldsymbol{x}}\left[\left[\mathcal{Y}_{L_1}(\widetilde{u}_1\boldsymbol{x})\mathcal{Y}_{L_2}(\widetilde{u}_2\boldsymbol{x})\right]_L\chi_S\right]_{JM_J}\eta_{TM_T}\right\}, \quad (1)$$

where $\mathcal{Y}_\ell(\boldsymbol{r}) = r^\ell Y_\ell(\widehat{\boldsymbol{r}})$ is a solid spherical harmonic. Here $\mathcal{A}$ is the antisymmetrizer, $\boldsymbol{x}$ is a column vector whose elements are three relative coordinates $(\boldsymbol{x}_1, \boldsymbol{x}_2, \boldsymbol{x}_3)$, and A is a 3×3 positive-definite, symmetric matrix whose six independent elements are variational parameters. The vectors u_1 and u_2 each contain three elements determining the weightings of the relative coordinates and are used to specify the angular motion of the basis (1). The tilde stands for the transpose of a column vector, and thus the inner product $\widetilde{u}_1\boldsymbol{x}$, which we call a global vector, is a vector in three-dimensional coordinate space. However, the inner product $\tilde{\boldsymbol{x}}A\boldsymbol{x}$ denotes a scalar in three-dimensional space as it is defined by $\sum_i \boldsymbol{x}_i\cdot(A\boldsymbol{x})_i = \sum_{i,j} A_{ij}\boldsymbol{x}_i\cdot\boldsymbol{x}_j$.

The global vector representation for the rotational motion used in Eq. (1) is found to be very useful. The reader is referred to Refs. [12] and [13] for more details. The spin function χ_{SM_S} in Eq. (1) is specified in a successive coupling, $[[[\frac{1}{2}\frac{1}{2}]_{S_{12}}\frac{1}{2}]_{S_{123}}\frac{1}{2}]_{SM_S}$, and all possible intermediate spins (S_{12}, S_{123}) are taken into account in the calculation. The isospin function η_{TM_T} is also treated in exactly the same way as the spin function. For both $T = 0$ and 1, the states with spin-parity J^π are obtained including in Eq. (1) the following (LS) values:

J^π	(LS)
0^+	(00), (22) ; (11)
1^+	(01), (21), (22) ; (10), (11), (12), (32)
0^-	(11) ; (22)
1^-	(10), (11), (12), (32) ; (21), (22)
2^-	(11), (12), (31), (32) ; (20), (21), (22), (42).

Here the semicolon divides a natural-parity set from an unnatural-parity one. For a given L, the values of L_1, L_2 in Eq. (1) are chosen to be $L, 0$ for natural parity and $L, 1$ for unnatural parity. Any basis functions with $L^\pi = 0^-$ are not included in the present calculation.

Each basis function differs in the choices of A, u_1, and u_2. The exponential part specified by A is called an explicitly correlated Gaussian. An alternative expression for this part is given using the single-particle coordinate $\boldsymbol{r}_i$ as [14]

$$e^{-\frac{1}{2}\tilde{\boldsymbol{x}}A\boldsymbol{x}} = \exp\left[-\frac{1}{2}\sum_{i<j}\left(\frac{\boldsymbol{r}_i - \boldsymbol{r}_j}{b_{ij}}\right)^2\right]. \quad (2)$$

Specifying the elements of A using the six variables $(b_{12}, b_{13}, \ldots, b_{34})$ is convenient for controlling the spatial extension of the system.

III. RESULTS

A. Energy spectrum

The accuracy of our solution depends on the basis dimension and the optimization of the variational parameters. The selection of the parameters is performed by the stochastic variational method [14,15]. As all the states but the ground state are resonances, increasing the basis size unconditionally does not always lead to a solution we are seeking. Namely, if the variational parameters are allowed to extend very far in the spatial region, the energy for the excited state would fall down to the $^3\mathrm{H} + p$ threshold.

Some details of the calculation are given below. The b_{ij} parameters in Eq. (2) are restricted to $0 < b_{ij} < 8$ fm for all the states but the 0^-1 state. This choice covers a configuration space large enough to obtain accurate solutions for both the ground and first-excited states [12]. Each element of u_i is allowed to take a value in the interval $[-1, 1]$ under the constraint that its norm is unity, i.e., $\widetilde{u}_i u_i = 1$. Note that changing the normalization of u_i does not actually alter the basis function (1) except for its normalization. We found that using 600 basis states of the form given in Eq. (1) (that is, 600 choices of parameters for A, u_1, u_2, L, S, S_{12}, S_{123}, T_{12}, T_{123}) enabled us to obtain converged solutions for both the ground and first-excited states. See Fig. 1 of Ref. [12]. Solutions for the other states are obtained in a basis dimension of 300. Figure 1 displays the energy convergence of the three lowest-lying negative-parity states with $J^\pi T = 0^-0, 2^-0$, and 2^-1 as a function of basis dimension. The energies of these states are rather stable with increasing basis size, though they do not have the proper asymptotic behavior characteristic of a resonance. The energies obtained for the higher levels, which present much larger widths, are not as accurate. Therefore, the results of our calculations for these states are more qualitative. In particular we found that the energy of the 0^-1 state, which has a width of about 8 MeV, was not as stable as the other states. We thus obtained its energy by restricting the range of b_{ij} to $0 < b_{ij} < 6$ fm.

Figure 2 compares the experimental and theoretical spectra of ^{4}He. The calculated binding energy of ^{3}H is 7.73 MeV for G3RS and 7.76 MeV for AV8′ [12]. Thus the calculated

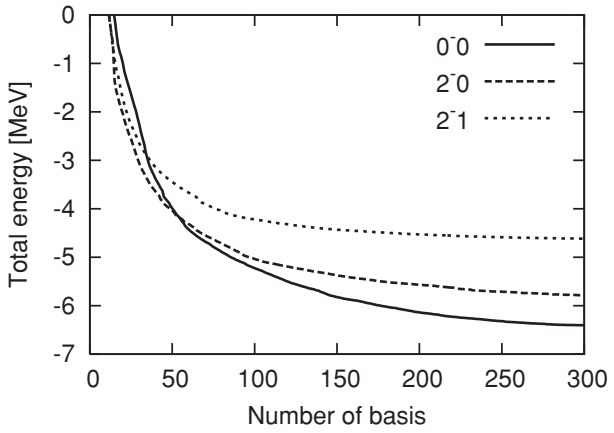

FIG. 1. The energy convergence of the three lowest-lying negative-parity states of ^{4}He calculated using the G3RS potential.

^{3}H + p threshold energy misses the experimental one by about 0.7 MeV. As we are interested in comparing the excitation spectra, the experimental and theoretical ^{3}H + p thresholds in the figure are drawn at the same level. The theory reproduces the level sequence of the spectrum as a whole and especially the excitation energies of the 0_2^+0, 0^-0, and 2^-0 states very well. The levels above $E_x = 23$ MeV are predicted to be slightly lower than experiment except for the 0^-1 level with AV8′. As their widths are all larger than 5 MeV, this discrepancy may be allowable in the bound-state approximation for unbound states. Noteworthy is that the calculation predicts three states with 0^+1, 1^+0, and 1^+1 around $E_x = 23$ MeV, as denoted by dashed lines. These states together with the 0_2^+0 state are the members of the quartet relevant to the first question. As speculated, they show up in the present calculation, but no such states are observed experimentally.

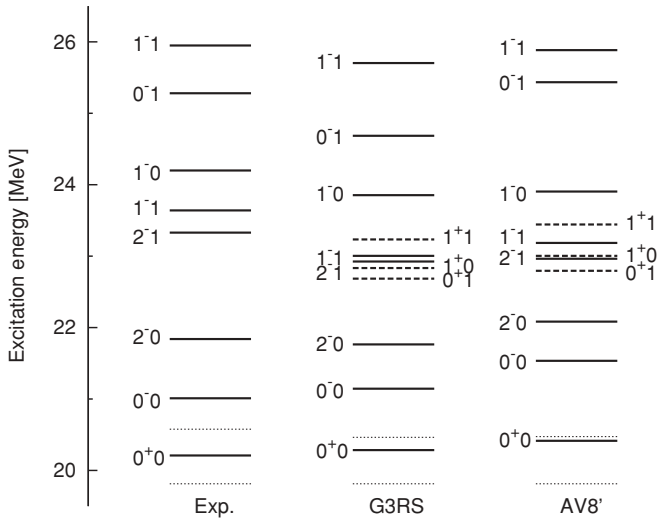

FIG. 2. Energy levels of the excited states of ^{4}He labeled with $J^\pi T$. Three states of the quartet are denoted by dashed lines. The dotted lines indicate the ^{3}H + p and ^{3}He + n thresholds, respectively. Experimental values are taken from Ref. [16].

TABLE I. Percentages of (LS) components of the quartet states calculated using the G3RS potential. Unnatural parity components are negligibly small.

	0_2^+0	0^+1	1^+0	1^+1
(00)	93.0	93.4	–	–
(01)	–	–	93.3	93.4
(21)	–	–	3.0	3.4
(22)	6.9	6.6	3.7	3.1

B. Quartet

To resolve the first problem on the quartet, we begin by understanding why only the 0_2^+0 state gets considerably lower than the other quartet members. As shown in Table I, all the members of the quartet consist of about 93% $L = 0$ components and 7% $L = 2$ components. These values are almost equal to the corresponding components in ^{3}H and ^{3}He [12], consistent with the conjecture that the quartet has $3N + N$ cluster structure with a relative S-wave motion.

We list in Table II the energy contributions to the quartet members. To this end we express the wave function $\Psi_{JM_JTM_T}$ of the quartet member as a sum of the components with different L values,

$$\Psi_{JM_JTM_T} = \Psi_0 + \Psi_2 + \Psi_1 + \cdots, \tag{3}$$

where Ψ_L includes the basis functions with all possible S values for a given L. For example, in the case of $J^\pi = 1^+$, Ψ_2 consists of the basis functions with $(LS) = (21)$ and (22). The matrix elements of the Hamiltonian H as well as those of its various components are shown in a matrix form in the table. The row and column labels of the 3×3 matrix correspond to the order of $L = 0, 2$, and 1. The $L = 3$ contributions are negligibly small and are omitted. The diagonal element indicates the value of $\langle\Psi_L|\mathcal{O}|\Psi_L\rangle$ for the operator $\mathcal{O}$, while the off-diagonal elements in the upper triangular part indicate the sum of $\langle\Psi_L|\mathcal{O}|\Psi_{L'}\rangle + \langle\Psi_{L'}|\mathcal{O}|\Psi_L\rangle$.

We see from the table that the key elements which give the 0_2^+0 state binding energy about 3 MeV larger than that of the other members are the kinetic energy as well as the tensor force. The kinetic energy contribution from the main channel listed in Table I is found to be about 2 MeV smaller in the 0_2^+0 state than in the other states. This is a consequence of the symmetry of the orbital part of the wave function as understood from Wigner's supermultiplet theory [17]. The spin and isospin function of four nucleons contains more numbers of antisymmetric pairs in the $S = 0, T = 0$ channel than in other ST channels, so that the orbital part of the 0_2^+0 state is more symmetric with respect to the nucleon exchange than the other orbital functions. Furthermore, the 0_2^+0 state gains about 1 MeV energy compared to the others states, due to the tensor coupling between the $L = 0$ and $L = 2$ components. In fact, it is interesting to realize from Tables I and II that the tensor force matrix element, $\langle\Psi_0|V_t|\Psi_2\rangle/\sqrt{\langle\Psi_0|\Psi_0\rangle\langle\Psi_2|\Psi_2\rangle}$, is -44.6 MeV. This large matrix element gives the Ψ_0 state the energy shift of about 12 MeV despite the fact the energy of the Ψ_2 state, $\langle\Psi_2|H|\Psi_2\rangle/\langle\Psi_2|\Psi_2\rangle$, is as high as 158 MeV.

TABLE II. Energy contributions to the total energies of the quartet states, given in MeV, and their decomposition into the contributions from the kinetic energy and the different potential pieces. The row and column of each 3×3 matrix correspond to the configuration spaces with $L = 0$, 2, and 1. See text for the details. The G3RS potential is used.

	$T=0$						$T=1$					
	0^+			1^+			0^+			1^+		
	4.58	−22.65	−0.00	6.48	−21.74	−0.01	6.30	−21.67	−0.00	6.62	−21.31	−0.01
H		10.97	−0.29		10.64	−0.16		10.58	−0.12		10.45	−0.15
			0.14			0.08			0.06			0.08
	29.26	–	–	31.09	–	–	31.45	–	–	31.73	–	–
T		10.99	–		10.30	–		10.31	–		10.08	–
			0.15			0.08			0.06			0.08
	−25.07	–	–	−25.00	–	–	−25.54	–	–	−25.50	–	–
V_c		−1.56	–		−1.26	–		−1.28	–		−1.17	–
			−0.01			−0.00			−0.00			−0.00
	0.39	–	–	0.39	–	–	0.39	–	–	0.40	–	–
$V_{\rm Coul}$		0.03	–		0.03	–		0.03	–		0.02	–
			0.00			0.00			0.00			0.00
	–	−22.65	–	–	−21.75	–	–	−21.67	–	–	−21.31	–
V_t		1.54	−0.30		1.61	−0.16		1.56	−0.13		1.55	−0.13
			0.01			0.00			0.00			0.00
	–	–	−0.00	–	–	−0.01	–	–	−0.00	–	–	−0.01
V_b		−0.02	0.00		−0.03	0.00		−0.05	0.00		−0.03	0.00
			0.00			0.00			0.00			0.00

Now we discuss whether or not the quartet states can be observed as resonances in $^3\mathrm{H}+p$ and $^3\mathrm{He}+n$ decay channels. To this end we calculate a spectroscopic (or reduced width) amplitude (SA) defined as

$$y(r) = \sqrt{\frac{4!}{3!}} \left\langle \left[\left[\Psi_{\frac{1}{2},\frac{1}{2}m_t}(3N) \phi_{\frac{1}{2},\frac{1}{2}-m_t}(N) \right]_I Y_\ell(\hat{\boldsymbol{R}}) \right]_{JM_J} \times \frac{\delta(R-r)}{Rr} \right| \Psi_{JM_JT0}(^4\mathrm{He}) \Big\rangle. \quad (4)$$

Here $\boldsymbol{R}$ is the $3N$-N relative distance vector, $\Psi_{1/2,1/2\,m_t}$ the normalized $3N$ ground-state wave function, and $\phi_{1/2,1/2\,-m_t}$ the nucleon spin-isospin function. They are coupled to the channel spin I. The label m_t distinguishes either $^3\mathrm{H}+p$ ($m_t = 1/2$) or $^3\mathrm{He}+n$ ($m_t = -1/2$) channel. The $3N$ wave function $\Psi_{1/2,1/2\,m_t}$ used here is obtained in the calculation using the basis of type (1) with $(LS) = (0\frac{1}{2})$ and $(2\frac{3}{2})$ [12]. The $L = 1$ component is very small (0.05%) and is ignored unless otherwise indicated. Figure 3 displays the $^3\mathrm{He}+n$ SAs of the quartet. The orbital angular momentum between the clusters is set to $\ell = 0$, and so I is equal to J. The $^3\mathrm{H}+p$ SA is virtually the same as the $^3\mathrm{He}+n$ SA (except for the phase). The 0_2^+0 state exhibits behavior quite different from that of the others in that its peak position of 3 fm is outside the $3N$ radius (~ 2.3 fm). Moreover, the spectroscopic factor, defined as $\int_0^\infty y^2(r) r^2 dr$, is very large with a value of 1.03. In a sharp contrast to the 0_2^+0 state, the SAs of the other quartet members show nothing of resonant behavior in that the peaks are located extremely far outside the $3N$ radius, and the y^2 value is small in the inner region. Therefore, we conclude that none of the quartet members except for the 0_2^+0 state is a physically observable resonance. This conclusion is consistent with the RGM phase-shift analysis, which finds no resonance around the 23 MeV excitation energy region [8]. In passing we note that the SA of the ground state has a sharp contrast with that of the 0_2^+ state in that the peak appears near the origin and the amplitude is confined mostly in the $3N$ radius.

Because our variational solution is expected to be fairly accurate at least in the inner region, a decay width can be estimated with an R-matrix type formula,

$$\Gamma_N = 2P_\ell(kr) \frac{\hbar^2 r}{2\mu} y^2(r), \quad (5)$$

where k is the wave number given by $k = \sqrt{2\mu E/\hbar^2}$ with the decay energy E, μ is the reduced mass of the decaying

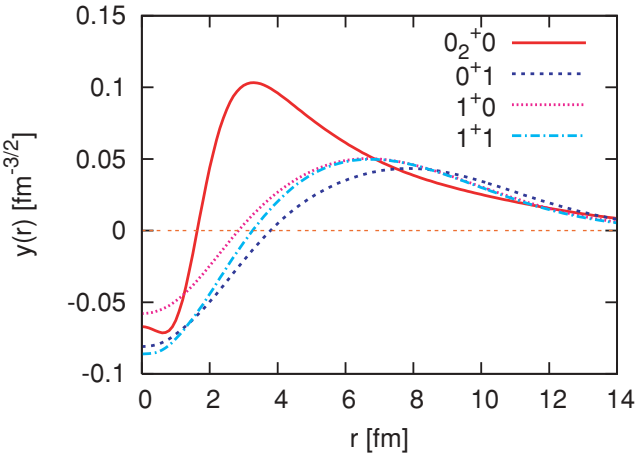

FIG. 3. (Color online) SAs of the quartet states for the S-wave $^3\mathrm{He}+n$ decay. The G3RS potential is used.

TABLE III. Percentage of (LS) components of the negative-parity states calculated using the G3RS potential. The natural and unnatural parity channels are separated by a rule.

(LS)	$T=0$			$T=1$			
	0^-	1^-	2^-	0^-	1^-_1	1^-_2	2^-
(10)	–	19.7	–	–	51.0	42.9	–
(11)	95.5	74.2	93.0	96.9	43.0	53.1	93.7
(12)	–	0.8	0.3	–	0.0	0.6	0.2
(31)	–	–	2.9	–	–	–	2.8
(32)	–	3.4	2.0	–	4.3	0.1	1.7
(20)	–	–	0.0	–	–	–	0.0
(21)	–	1.8	0.5	–	1.1	1.5	0.5
(22)	4.5	0.2	1.4	3.1	0.5	1.8	1.1
(42)	–	–	0.0	–	–	–	0.0

particles, and P_ℓ is the penetrability,

$$P_\ell(kr) = \begin{cases} \frac{kr}{F_\ell^2(kr)+G_\ell^2(kr)} & \text{for} \quad {}^3\mathrm{H}+p \\ \frac{kr}{(kr)^2[j_\ell^2(kr)+n_\ell^2(kr)]} & \text{for} \quad {}^3\mathrm{He}+n, \end{cases} \tag{6}$$

which is expressed in terms of either Coulomb wave functions or spherical Bessel functions. The decay width (5) depends on the channel radius r, but its dependence is found to be mild in that the Γ_p values of the $0^+_2 0$ state are 0.69, 0.74, and 0.67 MeV at $r = 4$, 5, and 6 fm, in good agreement with the empirical value of 0.50 MeV [16]. The above analyses all confirm that the $0^+_2 0$ state has a well-developed $3N + N$ cluster structure, in accordance with the conclusion of Ref. [4].

As discussed above, all the quartet members except for the $0^+_2 0$ state fail to gain enough energy to come down below the ${}^3\mathrm{He}+n$ threshold. The $0^+_2 0$ state actually shows up between the ${}^3\mathrm{H}+p$ and ${}^3\mathrm{He}+n$ thresholds thanks to their Coulomb energy difference. Isospin conservation leads to an almost equal mixing of the open $({}^3\mathrm{H}+p)$ and closed $({}^3\mathrm{He}+n)$ channels for the $0^+_2 0$ state. The effects of both the isospin conservation and the ${}^3\mathrm{H}+p$ Coulomb barrier make the Γ_p value of the $0^+_2 0$ state rather small. This state is thus a good example of a Feshbach resonance [18].

C. Negative-parity partners of the first excited 0^+ state

Before coming to the inversion doublet issue, we first comment on the features of the negative-parity states. According to the shell model, the negative-parity states basically arise from the $s^{-1}_{1/2}p_{3/2}$ or $s^{-1}_{1/2}p_{1/2}$ particle-hole excitation, which predicts $J^\pi = 0^-, 1^-, 1^-$, and 2^- for both $T = 0$ and 1. However, a particular combination of the two 1^- states with $T = 0$ corresponds to the state with the excitation of the center of mass, leaving only one intrinsically excited state with 1^- and $T = 0$. Seven negative-parity states observed experimentally below $E_x = 26$ MeV include three states with $T = 0$ and four states with $T = 1$, which is in agreement with the shell-model prediction. However, this agreement may not necessarily mean that the negative-parity states have shell-model like structure because the present four-body calculation also produces seven negative-parity states, as shown in Fig. 2.

The level sequence is $0^-, 2^-$, and 1^- in the order of increasing energy for $T = 0$, while it is $2^-1^-0^-$, and 1^- for $T = 1$. Therefore the energy difference between the 0^-0 and 0^-1 states becomes much larger than the one between the 1^-0 and 1^-1 states or between the 2^-0 and 2^-1 states. It is interesting to clarify the mechanism of how this large energy difference is produced compared to the other negative-parity states with the same J^π. Table III lists the percentage analysis of the seven negative-parity states according to their (LS) channels. The main component has $L = 1$ as expected from the shell model. Those states that have the same J^π but different T values present rather similar percentages. This similarity is not as clear in the case of the 1^- states, because in the $T = 1$ channel the strength is fragmented between two 1^-1 states. The main channel with $L = 1$ itself has a contribution from the tensor force but also gets a contribution from the other channels through the tensor coupling. For example, the tensor force couples the natural parity channel (11) with the unnatural parity channel (22).

Table IV lists the contributions to the energy from the various components of the Hamiltonian. Most striking are the different contributions from the tensor force. Compared to the 0^-1 state, the 0^-0 state gains about 9 MeV energy from the tensor force, while the contribution from the central force to the energy gain is only about half this. The energy contributions given by the AV8′ potential are similar to those of the G3RS potential: The gain from the tensor force is even larger, about 12 MeV, and the central force gives a 3 MeV difference. The tensor force is most attractive in the triplet even NN state, and it can be taken advantage of by having more antisymmetric NN pairs in the isospin space. The number of such antisymmetric pairs is obtained from $\langle \eta_{TM_T} | \sum_{i<j}(1-\boldsymbol{\tau}_i\cdot\boldsymbol{\tau}_j)/4 | \eta_{TM_T}\rangle$, which gives $[A(A+2)-4T(T+1)]/8$ for an A-nucleon system. Thus the 0^-0 state gains more attraction

TABLE IV. Energy contents, given in MeV, of the negative-parity states. The G3RS potential is used.

	0^-0	0^-1	2^-0	2^-1	1^-0	$1^-_1 1$	$1^-_2 1$
$\langle H\rangle$	−6.40	−2.86	−5.78	−4.62	−3.69	−4.54	−1.84
$\langle T\rangle$	48.38	39.10	41.08	40.25	37.72	39.30	32.48
$\langle V_c\rangle$	−28.92	−24.79	−25.71	−25.82	−23.50	−25.14	−22.01
$\langle V_{\mathrm{Coul}}\rangle$	0.48	0.44	0.42	0.43	0.40	0.43	0.42
$\langle V_t\rangle$	−26.63	−17.75	−21.39	−19.30	−18.32	−19.13	−12.67
$\langle V_b\rangle$	0.29	0.14	−0.18	−0.18	0.006	0.005	−0.06

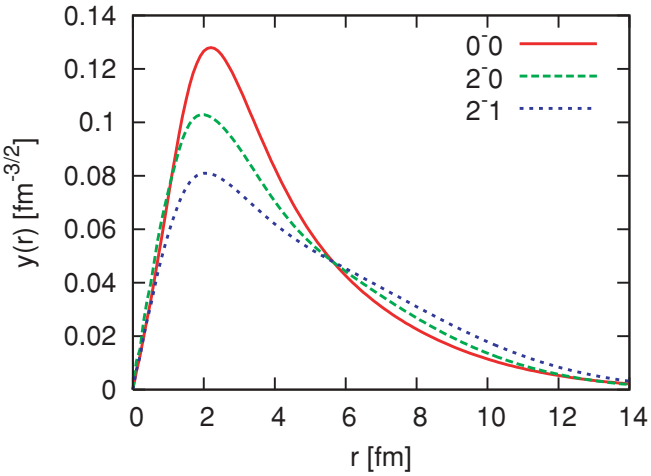

FIG. 4. (Color online) SAs of the three lowest-lying negative-parity states for the P-wave $^3\mathrm{He}+n$ decay with $I=1$. The G3RS potential is used.

than the 0^-1 state through both the (11)-(11) diagonal and (11)-(22) off-diagonal contributions [12]. If the unnatural parity basis states were not included in the calculation, the $\langle V_t\rangle$ value of the 0^-0 state would decrease to about half [12] and the 0^-0 state would lose significant energy. The role of the tensor force in lowering the energy of the 0^-0 state was discussed many years ago [5,19]. To be exact, the energy difference between the two states is actually a combined effect of the tensor, kinetic, and central terms.

Now we discuss the characteristics of the low-lying negative-parity states from the viewpoint of clustering. In Fig. 4 we display the $^3\mathrm{He}+n$ SAs calculated from the three lowest-lying negative-parity states with 0^-0, 2^-0, and 2^-1. The ℓ value for the $^3\mathrm{He}-n$ relative motion is 1, and the channel spin I is 1. As expected, each of the three curves shows behavior suggesting $3N+N$ cluster structure: The peaks are centered around 2 fm near the $3N$ surface, and the y^2 values are fairly large in the inner region. It is the centrifugal potential that makes the peak positions closer to the origin than for the first excited 0^+0 state. The $3N+N$ spectroscopic factors are quite large, being 0.58, 0.52, and 0.53 for the 0^-0, 2^-0, and 2^-1 states. When we estimate the nucleon width, the channel-radius dependence is again mild, so we choose $r=5$ fm. The results for $(\Gamma, \Gamma_p/\Gamma)$, where Γ is the total width in MeV, are (0.61, 0.72), (1.14, 0.58), and (1.85, 0.53) for 0^-0, 2^-0, and 2^-1, respectively. These values are to be compared to those extracted from the R-matrix analysis [16], (0.84, 0.76), (2.01, 0.63), and (5.01, 0.53). The theory predicts the width of the 0^-0 state very well and gives about half of the width for the other states. Though the degree of clustering is somewhat reduced in the negative-parity states compared to the 0^+_2 case, the analysis of SA and decay width supports our conjecture that the 0^-0 and 2^-0 states as well as the 2^-1 state constitute inversion-doublet partners of the first excited 0^+ state. The RGM phase-shift analysis of $^3\mathrm{H}+p$ scatterings [8] supports the P-wave resonance interpretation for these negative-parity states. The SAs of the 1^- states around $E_x=24$ MeV show some degree of $3N+N$ cluster structure, though their amplitudes are considerably smaller compared to the 0^-0 and 2^-0 states in particular.

An inversion doublet picture in nuclei was first proposed to understand the low-lying positive- and negative-parity rotation bands in ^{16}O and ^{20}Ne from an α-core molecular structure [20]. The appearance of positive- and negative-parity partners is a natural consequence of the underlying intrinsic structure dominated by the existence of asymmetric clusters. We have shown that the three lowest-lying negative-parity states have a significant component of $3N$ and N clusters whose relative motion is in P wave. It is important to realize that this result is obtained in a calculation that assumes no cluster ansatz for the wave functions. A physical reason for the appearance of the inversion doublet partners is that they are located near the $3N+N$ threshold.

Very unique to the inversion doublets in ^{4}He is that the $3N$ and N clusters have both $J=1/2$, and the channel spin I is different in the doublets: It is 0 for $0^+_2 0$ and 1 for 0^-0, 2^-0, and 2^-1. The negative-parity partners with $T=0$ should thus be characterized by an isoscalar spin-dipole operator, $\mathcal{O}_{\lambda\nu}=\sum_{i=1}^4[\boldsymbol{\sigma}_i\times(\boldsymbol{r}_i-\boldsymbol{x}_4)]_{\lambda\nu}$, where $\boldsymbol{x}_4$ is the center of mass of ^{4}He, connecting them to the 0^+_2 state. Note that $\boldsymbol{r}_i-\boldsymbol{x}_4$ is proportional to the distance vector between nucleon i and the center of mass of the other three nucleons. The transition strength to the $0^+_2 0$ state, $|\langle 0^+_2 0||\mathcal{O}_0||0^-0\rangle|^2$, is 11.9 fm^2, which is 6.9 times larger than that to the ground state. Moreover, the strength $|\langle 0^+_2 0||\mathcal{O}_0||0^-0\rangle|^2$ between the doublet partners occupies 58% of the "sum rule" $\sum_n|\langle 0^+_n 0||\mathcal{O}_0||0^-0\rangle|^2$, where n takes all 600 eigenstates with 0^+0. A similar enhancement occurs for the 2^-0 state as well. The value $|\langle 0^+_2 0||\mathcal{O}_2||2^-0\rangle|^2/5$ is 21.7 fm^2, which is about 24 times larger than the one to the ground state, and it corresponds to 78% of the total sum $\sum_n|\langle 0^+_n 0||\mathcal{O}_2||2^-0\rangle|^2/5$.

For the transition between the 2^-1 and $0^+_2 0$ states, an isovector spin-dipole operator, $\mathcal{O}_{\lambda\nu,10}=\sum_{i=1}^4[\boldsymbol{\sigma}_i\times(\boldsymbol{r}_i-\boldsymbol{x}_4)]_{\lambda\nu}\tau_{3_i}$, must be considered. The transition strength $|\langle 0^+_2 0|||\mathcal{O}_{2,1}|||2^-1\rangle|^2/15$ is 17.4 fm^2, which is 16 times larger than that to the ground state, where the triple bar indicates that the reduced matrix element is taken in both the angular momentum and isospin spaces. This strength between the 2^-1 and $0^+_2 0$ states accounts for 87% of the total strength $\sum_n|\langle 0^+_n 0|||\mathcal{O}_{2,1}|||2^-1\rangle|^2/15$.

The high collectivity of the spin-dipole strength strongly indicates that the intrinsic structure of the negative-parity states, 0^-0, 2^-0, and 2^-1, is similar to that of the first excited $0^+_2 0$ state.

IV. SUMMARY

A rich portion of the ^{4}He spectrum, including levels in which particle-hole and cluster excitations coexist, has been reproduced in a single scheme without recourse to the assumption of a specific model. This has offered a good demonstration of the power of the global vector representation for the angular part for few-body systems. We have explained how only the 0^+_2 state is observed as a resonance among the quartet states by examining the symmetry property of the wave functions as well as the role of the tensor force. By

analyzing the spectroscopic amplitudes, nucleon decay widths, and spin-dipole transition probabilities, we have confirmed that both the 0_2^+ and negative-parity states with 0^-0, 2^-0, and 2^-1 are dominated by a $3N + N$ cluster structure and that these negative-parity states can be understood as the inversion-doublet partners of the 0_2^+ state in a unified way. We have shown that the tensor force plays a vital role to reproduce the level spacing between the 0^- states with $T = 0$ and 1 through the coupling between the main channel with $L = 1$ and the unnatural-parity channel with $L = 2$. A study of ^{16}O in the scheme of ^{12}C plus four nucleons will be interesting because its spectrum has some similarity to that of ^{4}He.

ACKNOWLEDGMENTS

The authors are greatly indebted to D. J. Millener for his careful reading of the manuscript and useful comments. This work was in part supported by a Grant for Promotion of Niigata University Research Projects (2005-2007) and by a Grant-in Aid for Scientific Research for Young Scientists (No. 19·3978). W.H. is supported by the JSPS research program for young scientists. Y.S. thanks the JSPS core-to-core program (Exotic Femto Systems) and the Institute for Nuclear Theory at the University of Washington for the support which enabled him to have useful communications in the INT Workshop on Correlations in Nuclei, November 2007.

[1] M. Chernykh, H. Feldmeier, T. Neff, P. von Neumann-Cosel, and A. Richter, Phys. Rev. Lett. **98**, 032501 (2007), and see also references therein.
[2] P. Navrátil, J. P. Vary, and B. R. Barrett, Phys. Rev. Lett. **84**, 5728 (2000).
[3] Y. Suzuki, Prog. Theor. Phys. **55**, 1751 (1976); **56**, 111 (1976).
[4] E. Hiyama, B. F. Gibson, and M. Kamimura, Phys. Rev. C **70**, 031001(R) (2004).
[5] M. Sakai, Y. Akaishi, and H. Tanaka, Prog. Theor. Phys. Suppl. **56**, 108 (1974).
[6] P. Navrátil and B. R. Barrett, Phys. Rev. C **59**, 1906 (1999); **54**, 2986 (1996).
[7] A. Csótó and G. M. Hale, Phys. Rev. C **55**, 2366 (1997).
[8] H. M. Hofmann and G. M. Hale, Nucl. Phys. **A613**, 69 (1997); Phys. Rev. C **77**, 044002 (2008).
[9] J. Carlson, V. R. Pandharipande, and R. B. Wiringa, Nucl. Phys. **A424**, 47 (1984).
[10] R. Tamagaki, Prog. Theor. Phys. **39**, 91 (1968).
[11] R. B. Wiringa, V. G. J. Stoks, and R. Schiavilla, Phys. Rev. C **51**, 38 (1995).
[12] Y. Suzuki, W. Horiuchi, M. Orabi, and K. Arai, Few-Body Syst. **42**, 33 (2008).
[13] Y. Suzuki, J. Usukura, and K. Varga, J. Phys. B **31**, 31 (1998); K. Varga, Y. Suzuki, and J. Usukura, Few-Body Syst. **24**, 81 (1998).
[14] Y. Suzuki and K. Varga, *Stochastic Variational Approach to Quantum-Mechanical Few-Body Problems*, *Lecture Notes in Physics Monographs* (Springer, Berlin, 1998), Vol. m54.
[15] K. Varga and Y. Suzuki, Phys. Rev. C **52**, 2885 (1995).
[16] D. R. Tilley, H. R. Weller, and G. M. Hale, Nucl. Phys. **A541**, 1 (1992).
[17] E. Wigner, Phys. Rev. **51**, 106 (1937).
[18] H. Feshbach, Ann. Phys. (NY) **5**, 357 (1958); **19**, 287 (1962).
[19] B. R. Barrett, Phys. Rev. **154**, 955 (1967).
[20] H. Horiuchi and K. Ikeda, Prog. Theor. Phys. **40**, 277 (1968).